

# Nanometer-Scale Organization of Ethylene Oxide Surfactants on Graphite, Hydrophilic Silica, and Hydrophobic Silica

Lachlan M. Grant,<sup>†</sup> Fredrik Tiberg,<sup>‡</sup> and William A. Ducker<sup>\*,†,§</sup>

Department of Chemistry, University of Otago, Dunedin, New Zealand, Institute for Surface Chemistry, Stockholm, Sweden, and Department of Chemistry, Virginia Tech, Blacksburg, Virginia

Received: November 19, 1997; In Final Form: March 12, 1998

To better understand the role of the interactions between surfactant, solvent, and a solid substrate on surface aggregation, we have studied the adsorption of a series of alkylpoly(ethylene oxide)  $C_nE_m$  surfactants on three different substrates: graphite, hydrophilic silica, and hydrophobic silica. Using atomic force microscopy (AFM), we find that adsorption to hydrophilic silica, with two exceptions, results in the formation of globular structures that are similar to bulk micelles. On silica that has been made hydrophobic by reaction with organosilane, adsorption results in a surface layer that is laterally homogeneous and is probably a monolayer with ethylene oxide groups in contact with the solution. A number of surfactants with ionic and zwitterionic headgroups were also observed to form monolayers on hydrophobic silica. This large perturbation from the solution-aggregate structure on the hydrophobic surface is driven by a minimization of the area of contact between water and the hydrophobic silica substrate. On graphite, the surface layer is either long, thin aggregates (consistent with a hemicylindrical structure) or a laterally homogeneous layer (consistent with a monolayer with the headgroups facing the solution). The nonionic  $C_{12}$  and  $C_{14}$  surfactants form hemicylinders, and the  $C_{10}$  surfactants with the same headgroups form a laterally homogeneous layer. This suggests that above a critical alkyl chain length the interaction between the graphite and the surfactant tail is sufficient to orient a layer of alkyl tail groups parallel to the graphite surface, which then templates further adsorption. Below the critical alkyl length, the arrangement on graphite is similar to that on hydrophobic silica and is probably driven by a minimization of the water–graphite interfacial area. The critical alkyl length for (zwitterionic) sulfobetaine surfactants is not the same as for the nonionic poly(ethylene oxide) surfactants. This shows that the headgroup also plays an important role in determining the adsorbed structure. All measurements were performed in equilibrium with bulk micelles at or above the critical micelle concentration and at approximately 25 °C.

## Introduction

Surfactant molecules often aggregate at solid–liquid interfaces, and the shape of these aggregates can be different from those in bulk solution.<sup>1</sup> Recently, the role of the solid phase in causing these changes has been examined via atomic force microscopy, particularly for graphite, which is a convenient substrate for microscopic studies.<sup>2–5</sup> It has been suggested that graphite exerts two major influences on the adsorbate geometry: a specific interaction due to epitaxy of the alkyl chain with the graphite crystal<sup>4,6</sup> and a nonspecific hydrophobic interaction between the water and graphite which drives a minimization of the graphite–water interfacial area.<sup>3,7</sup> In this paper we seek to explore these mechanisms by examining the aggregation of a variety of poly(ethylene oxide) surfactants at the interface between micellar solutions and solid substrates. Adsorption of these surfactants has been investigated by ellipsometry.<sup>8</sup> To test the influence of specific epitaxial binding of the alkyl chain, we have investigated surface aggregation as a function of alkyl chain length. To separate the hydrophobic effect from forces specific to graphite, we have compared the structure on graphite to the structure on silica that has been

made hydrophobic by reaction with diethyloctylchlorosilane (DEOS). To compare organization on a hydrophilic substrate to adsorption on a hydrophobic substrate, we have compared adsorption on hydrophobic silica to adsorption on hydrophilic silica. Hydrophilic silica contains silanol groups that interact with poly(ethylene oxide) headgroups through a nontrivial, weak interaction that includes hydrogen bonding. For the hydrophobic DEOS-silica, most of the hydrogen-bonding sites have been occupied by the diethyloctylchlorosilane, and the substrate is covered in alkyl chains. Thus, in terms of surfactant binding we wish to compare substrates that specifically interact with the headgroup (silica) or the alkyl chain (graphite) or to neither the surfactant nor the solvent (hydrophobic DEOS-silica).

## Experimental Section

**Sample Preparation and Characterization.** Water was purified by distillation then passage through a Milli-Q RG system consisting of charcoal filters, ion-exchange media, and a 0.2  $\mu\text{m}$  filter. The resulting water had a conductivity of 18  $\text{M}\Omega\text{ cm}^{-1}$  and a surface tension of 72.4  $\text{mJ m}^{-2}$  at 22.0 °C.

Penta(oxyethylene) *n*-decyl ether ( $C_{10}E_5$ ), obtained 97% pure from Sigma Chemicals, was used without further purification. Other monodisperse polyoxyethylene glycol alkyl ethers ( $C_{12}E_5$ ,  $C_{12}E_8$ ,  $C_{10}E_6$ ,  $C_{14}E_6$ , and  $C_{16}E_6$ ) were manufactured by Nikko Chemicals (Japan) and used without further purification. Hexa-

\* For correspondence, wducker@chemserver.chem.vt.edu.

<sup>†</sup> University of Otago.

<sup>‡</sup> Institute for Surface Chemistry.

<sup>§</sup> Virginia Tech.

**TABLE 1: Structure of  $C_nE_m$  Surface Aggregates<sup>a</sup>**

$C_nE_m$	cmc/mM	conc/cmc	hydrophilic silica	hydrophobic DEOS-silica	(hydrophobic) graphite
$C_{10}E_5$	0.81	5.3	globular	X <sup>a</sup>	continuous
$C_{10}E_6$	0.90	2.2	globular	continuous	continuous/hemicylinders (two phase)
$C_{12}E_5$	0.057	1.9	continuous/globular (force sensitive)	continuous	hemicylinders
$C_{12}E_8$	0.092	2.0	globular	continuous	X
$C_{14}E_6$	0.010	5.0	continuous/globular (force sensitive)	continuous	hemicylinders
$C_{16}E_6$	0.0017	2.0	globular	continuous <sup>b</sup>	X

<sup>a</sup> X = not measured. <sup>b</sup> Measured at the  $C_{16}E_6$  cmc.

decyltrimethylammonium bromide (CTAB), 99% (BDH, Poole, U.K.), was recrystallized three times from a distilled-acetone/water mixture. Dodecyldimethylammoniopropanesulfonate (DDAPS), 98% (Aldrich Chemicals, WI), was recrystallized from distilled 2-propanol. Lithium perfluorooctanesulfonate (LiFOS) was prepared by ion-exchange of KFOS (PCR, Gainesville, FL) on the  $H^+$  form of a Dowex column at 65 °C, neutralization with LiOH, then recrystallization twice from a mixture of distilled ethanol and distilled chloroform.

Solid substrates were prepared in the following manner.

**Graphite:** Adhesive tape was used to cleave along the basal plane of graphite from a pyrolytic graphite monochromator (grade ZYH, Union Carbide).

**Silica:** Silicon test slides (Okmetic) were oxidized thermally in a saturated oxygen atmosphere at 920 °C for 1 h, followed by annealing and cooling in an argon flow. This procedure results in a  $SiO_2$  layer with a thickness of about 30 nm. The wafers were cleaned in a mixture of 25%  $NH_4OH$ , 30%  $H_2O_2$ , and  $H_2O$  (1:1:5, by volume) at 80 °C for 5 min and subsequently rinsed in distilled water and then in ethanol. These silica wafers were exposed to UV irradiation for 40 min (about 9 mW  $cm^{-2}$  at 253.7 nm) immediately prior to use. We tested the effectiveness of the UV irradiation in removing organic material by UV irradiating the diethyloctylchlorosilane-silica. After UV irradiation, the adsorbed surfactant structures were the same as those formed on hydrophilic silica and different from those formed on hydrophobic DEOS-silica. The water contact angle was about 5°.

**Hydrophobic DEOS-silica:** The hydrophilic silica substrates were placed in a reactor containing diethyloctylchlorosilane (DEOS). Air was evacuated from the reactor by means of a water suction pump during the first 5 min of the dimethyloctylchlorosilane exposure. The water contact angles were  $\theta_{adv} = 105^\circ$  and  $\theta_{rec} = 95^\circ$ .

**Microscopy.** Images were captured using a Nanoscope III AFM<sup>9</sup> (Digital Instruments, CA) using silicon ultralevers (Park Scientific, CA) with spring constants of  $0.12 \pm 0.02$   $Nm^{-1}$ , as determined by measuring the resonant frequency of loaded and unloaded cantilevers.<sup>10</sup> The ultralevers were irradiated for 40 min (about 9 mW  $cm^{-2}$  at 253.7 nm) in a laminar flow cabinet before use. The images presented are deflection images (showing the error in the feedback signal) with low integral and proportional gains and scan rates of about 10 Hz. The only filtering of images was a linear subtraction from each line and the filtering inherent in the feedback loop. Distances in lateral dimensions were calibrated by imaging a standard grid (2160 line  $mm^{-1}$ ), and distances normal to the surface were calibrated by measuring etch pits (180 nm deep).

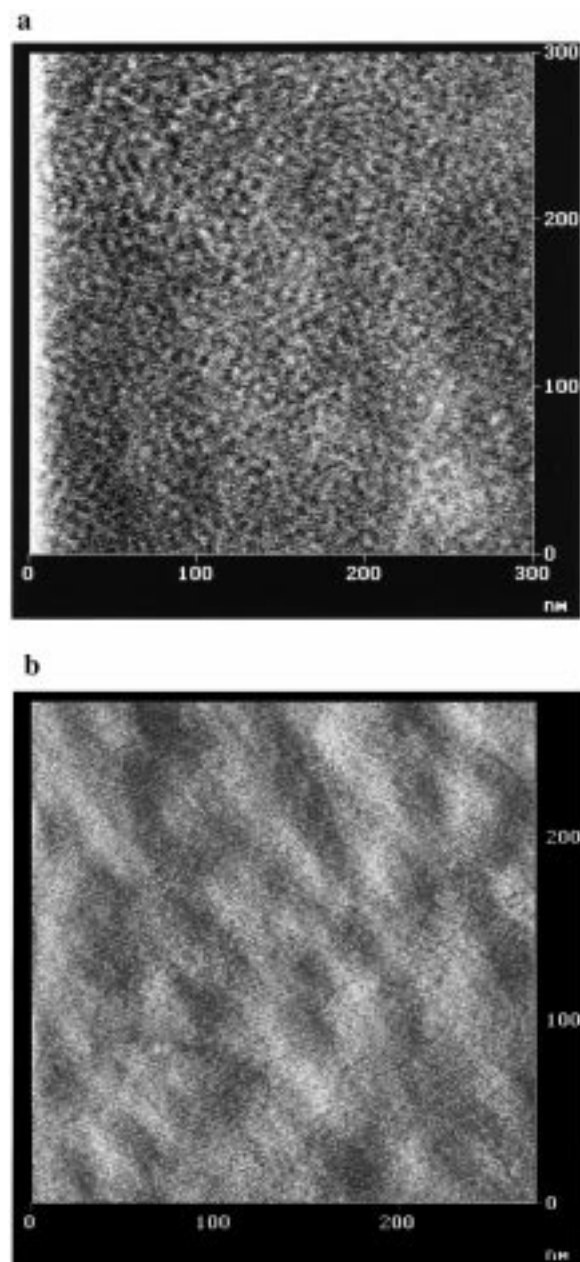
All measurements were performed in the temperature range  $25 \pm 2$  °C and in contact with single-phase surfactant solutions. Before images were captured each substrate/solution combination was left to equilibrate for at least 30 min and was then monitored for at least 2 h. We did not observe changes in structure over this period. Solutions were changed by flushing the AFM cell with about 20 times its volume of new solution

over 5 min. Each combination of surfactant and substrate was investigated at least twice, and between each surfactant solution, the AFM cell was flushed with water until a characteristic water curve was obtained. When surfactants were added in a different order, the same results were obtained. Imaging was performed at a force and separation at which the force on the tip was dominated by the surfactant film, and thus the image provided information about the surfactant film.

The forces between the tip and sample were also measured using a Nanoscope III AFM and analyzed as described previously.<sup>11</sup> It is important to note that the zero of separation is defined to occur when the gradient of the force has a high and constant (negative) value, which implies that the tip is in contact with the sample. Very strongly adsorbed material may not be displaced in a particular measurement, and therefore there may be a systematic error in evaluating the zero of separation for each complete measurement of force as a function of separation. The zero of force is defined to occur when the gradient in force is very low at a large separation.

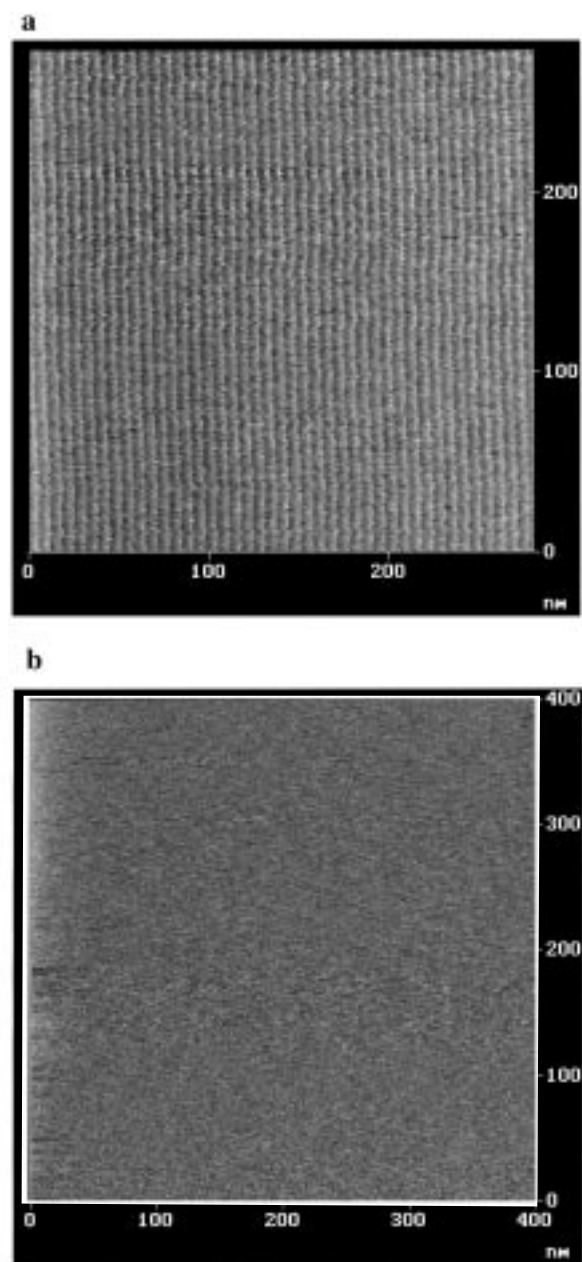
## Results

Table 1 is a summary of the structures observed for a variety of poly(ethylene oxide) surfactants on hydrophilic silica, hydrophobic DEOS-silica, and graphite. Globular surface micelles with center-center distances of about 7 nm are the main feature observed on hydrophilic silica, and a laterally homogeneous layer is always observed on hydrophobic DEOS-silica. These structures are shown for  $C_{12}E_8$  in Figure 1. This figure directly demonstrates that the curvature of the adsorbed surfactant aggregates is lower on a hydrophobic substrate. This supports our hypothesis that when water has a low affinity for the substrate, the surfactant forms low-curvature aggregates (in this case a flat sheet) which minimize the contact of water with the substrate, whereas when water has a high affinity for the substrate, the nonionic aggregate structure is similar to that found in bulk solution. Other surfactants also form continuous layers on hydrophobic DEOS-silica. We have found that sodium dodecyl sulfate (SDS) (anionic), hexadecyltrimethylammonium bromide (CTAB) (cationic), dodecyldimethylammoniopropanesulfonate (DDAPS) (zwitterionic), and lithium perfluorooctanesulfonate (LiFOS) (fluorocarbon) all form flat sheet structures on hydrophobic DEOS-silica, so it appears to be a general phenomenon. Previously, DDAPS has been shown to form spherical micelles on mica or silicon nitride<sup>2,3</sup> (both of which are hydrophilic), and CTAB has been found to form spherical micelles on silica<sup>4</sup> (which is hydrophilic); so both of these surfactants also fit the pattern of lower curvature aggregates on a hydrophobic substrate. Surfactants which have a much higher affinity than the solvent for the substrate (e.g., thiols on gold or charged surfactants on oppositely charged substrates) will not necessarily fit this pattern, as the high affinity of the surfactant for the substrate may lead to a flattening of the surface micelle to increase the contact between the headgroups and the substrate.<sup>12</sup>



**Figure 1.** AFM image of the association of  $C_{12}E_8$  molecules at the interface between a  $2 \times$  cmc solution and (a) hydrophilic silica or (b) hydrophobic diethyloctylsilane-silica. Light areas represent high regions or regions of greater repulsive force. On hydrophilic silica,  $C_{12}E_8$  associates into globular structures similar to micelles with center-to-center separations of  $6.5 \pm 0.5$  nm, and on the hydrophobic substrate, no micellar aggregates are observed. The constant-force surface above the hydrophobic silica shows some features on a scale of about 50 nm. These features are very similar to those on the underlying substrate, but adsorption of the surfactant has made the surface flatter. Adsorption of  $C_{10}E_5$ ,  $C_{10}E_6$ , and  $C_{16}E_6$  on hydrophilic and hydrophobic DEOS-silica produces very similar AFM images.

Graphite is also a hydrophobic substrate, but the aggregation behavior is more complicated than on hydrophobic DEOS-silica. For the  $C_nE_m$  surfactants, we find that when the alkyl chain length is 12 or 14 carbon-units long, then the surfactant forms discontinuous structures which are probably hemicylinders, but that when the alkyl chain is 10 carbon-units long, the surfactants form a laterally homogeneous (flat) layer (Figure 2). Cylindrical structures were occasionally observed in small patches (less than  $4 \times 10^4$  nm<sup>2</sup>) on the graphite in contact with  $C_{10}E_6$  solutions. This dilute inclusion of another structure is probably a two-



**Figure 2.** (a) AFM image of the organization of  $C_{14}E_6$  on graphite. The molecules associate into aggregates which have one dimension that is about 6 nm and the other is very long, usually at least 300 nm. The image shows the long axis perpendicular to the scan axis, but the same structure occurs at other imaging angles. Very similar structures are observed for  $C_{12}E_5$ . (b) AFM image of the organization of  $C_{10}E_6$  on graphite: the surfactant forms a continuous, flat film. A very similar structure is observed for  $C_{10}E_5$ . The structure is smoother than that formed on hydrophobic DEOS-silica, but the graphite is atomically smooth, whereas the hydrophobic DEOS-silica is rougher than the surface of the surfactant film that forms on it.

phase region of a very small amount of the hemicylindrical phase coexisting with the flat phase. Previously STM measurements of alkanes adsorbed to graphite have shown that the alkane chains lie in ordered arrays (lamellae) on the graphite surface.<sup>6</sup> It is hypothesized that this arrangement is due to a fortuitous match in the distance between the centers of the hexagonal graphite lattice and the distance between alternate methylene groups in the alkyl chain. The relationship between the lamellae axis and the alkyl chain orientation depends on the nature of other chemical groups attached to the alkyl chain.<sup>6</sup> It is reasonable to expect that this ordering effect scales with

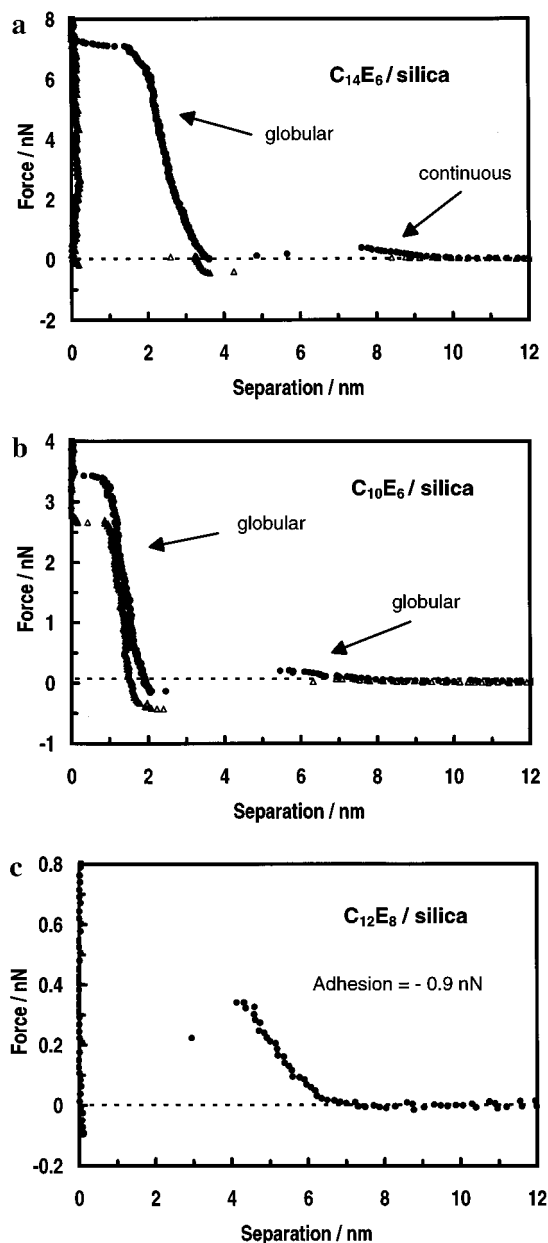


**Figure 3.** Force between an oxide-coated silicon AFM tip and silica in PEO solutions above the cmc. (a)  $C_{14}E_6$ . The closed circles show the force as the tip approaches the silica and indicate repulsion at about 7.5–9 nm. At this separation the constant-force surface is laterally homogeneous, which implies that the surfactant forms a homogeneous film. At a separation of about 4 nm, there is also a repulsive force. As the force is increased from this point, globular aggregates are observed with increasing resolution as the film is compressed. We interpret this as the compression of the surface micelles. The image symmetry does not change during this compression. The film of surfactant becomes much more compressible when it thins below 1.5 nm, but the thinning appears to be continuous. We interpret this high-compliance region as the displacement of the aggregate (probably laterally). The arrows indicate the image conditions for Figure 7, and the open triangles are the force measurements as the tip is separated after contact with the substrate. (b)  $C_{10}E_6$ . The force curve is similar to that measured for  $C_{14}E_6$  except (1) globular micelles are observed at all separations and (2) the repulsive force walls are shifted to smaller separations. Very similar behavior was observed for  $C_{16}E_6$ , except that for  $C_{16}E_6$  the steep repulsive force starts at greater separations (3 nm vs 2 nm) probably because of the longer hydrocarbon chain. (c)  $C_{12}E_8$ . For  $C_{12}E_8$ , we observed only one stable imaging position at separations from about 6.5 to 4 nm. Globular micelles were observed at this condition.

the length of the hydrocarbon chain. Thus, for surfactant adsorption in water, the first layer of the longer-chain  $C_{12}$  and

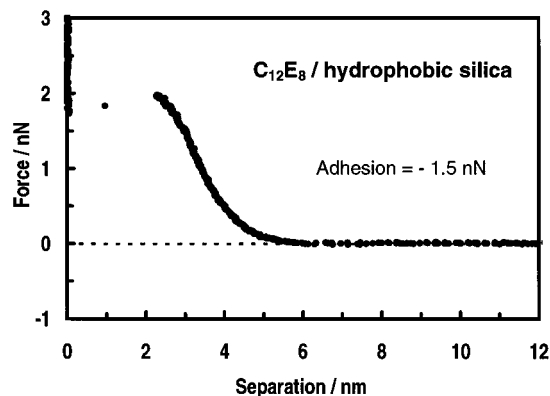


**Figure 4.** Force between an oxide-coated silicon AFM tip and hydrophobic DEOS-silica in  $C_nE_m$  surfactant solutions above the cmc. All the surfactants produced similar force curves on hydrophobic DEOS-silica. There was just one continuous repulsive force, then a tip instability that we attribute to the tip pushing through to the underlying substrate. On silica, the surfactant forms a discontinuous film, so there is the possibility of aggregates gradually moving laterally under normal pressure. Because the film is continuous on the hydrophobic substrate, there is no possibility of pushing aggregates to one side, so the film must rupture discontinuously.

$C_{14}$  surfactants form in long ribbons of tail-to-tail structures templated by the graphite surface. This ribbon structure then provides a template for the formation of a hemicylindrical structure. Recently Patrick et al.<sup>5</sup> have also found that the  $C_{12}E_m$  surfactants form hemicylindrical structures, except for  $C_{12}E_{23}$ , which forms a laterally homogeneous layer. They have shown that the axis of the hemicylinders is normal to the graphite crystal axes. For the shorter chain  $C_{10}$  surfactants, the ordering imposed by registry of the hydrocarbon chain with the graphite should be weaker, and we observe that the adsorbed layer is laterally homogeneous as for the hydrophobic DEOS-silica. We conclude that the layer of surfactant next to the graphite surfactant is not sufficiently ordered to template a hemicylindrical structure, or perhaps does not even predominantly lie parallel to the graphite interface. Further evidence for the weaker adsorption of the  $C_{10}$  alkyl chain is presented later (Figure 5). The appearance of a small amount of cylindrical structure for  $C_{10}E_6$  may indicate that there is a delicate balance between the surface-induced order driving the surfactant into cylindrical geometry and the high water–graphite interfacial energy driving the surfactant to form a continuous layer over the graphite.

The observed trend of a more curved structure (flat–hemicylinder transition) with increasing alkane content is the opposite of what is expected from a packing parameter argument.<sup>13</sup> In bulk solution, one would expect a greater volume of hydrocarbon (larger  $n$ ) to favor less curved aggregates. The fact that the opposite trend occurs on graphite is an indication of the strong templating effect of the first layer of surfactant on the remainder of the aggregate.

We have tested the concept of a critical alkyl length for a different headgroup, the zwitterionic ammoniopropanesulfonate group. Both the  $C_{10}$  and  $C_{12}$  surfactant form hemicylindrical structures on graphite, so clearly the headgroup interaction with water and graphite also plays a role in determining the surface-aggregate structure. The zwitterionic group has a much larger dipole moment than the polar groups in  $C_nE_m$  surfactants, so it can form a much stronger dipole/induced-dipole force with the graphite. (Graphite is conducting in the plane of the surface.) This may be the reason for the increased tendency of the zwitterionic surfactants to lay flat on the graphite surface.

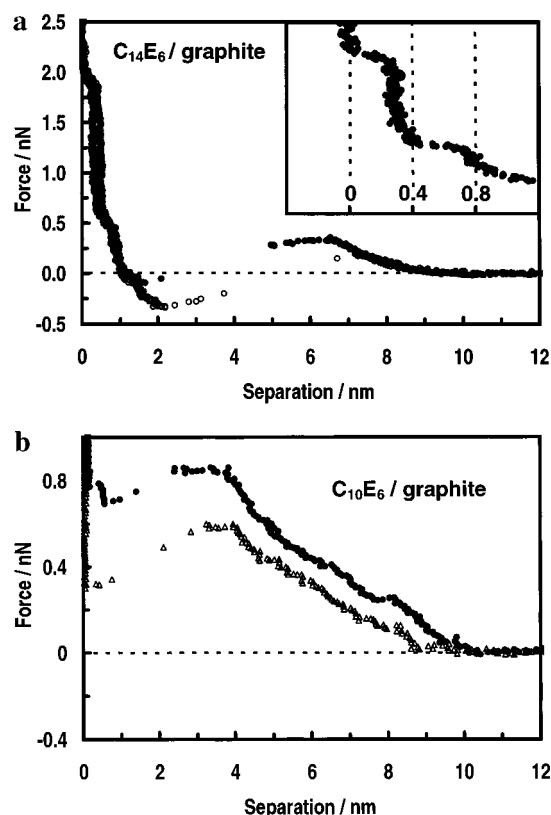


**Figure 5.** Force between an oxide-coated silicon AFM tip and graphite in  $C_nE_m$  solutions above the cmc. For all the surfactants the force curves were quite variable, but the force always shows thicker films than would be expected from a single adsorbed layer between the tip and sample. (a)  $C_{14}E_6$ . Note the very stable imaging position at a separation of about 0.3–0.4 nm shown in the inset. This is about the appropriate thickness for a single hydrocarbon chain lying flat on the graphite surface. A large force is required to remove this layer. There is also a force barrier at 0.8 nm, suggesting that there may be a second layer of molecules lying parallel to the graphite surface. (b)  $C_{10}E_6$ . There is also a repulsive force at 0.3–0.4 nm, but the magnitude is much smaller, and often this force was entirely absent. The difference in binding of the first layer of surfactant is illustrated by the fact that, for  $C_{10}E_6$ , the force required to remove the thin 0.3–0.4 nm layer is about the same as to remove the entire thick layer, whereas, for  $C_{14}E_6$ , the force required to remove the thin layer is about 3.5 times greater than the force required to remove the thick surfactant layer.

An interesting feature of surfactant adsorption to solid substrates is that the observed structure is often a function of the force applied by the tip. When the tip is withdrawn from the film (and the force is reduced to zero), the image returns to the unperturbed state within about a minute. Sometimes it is difficult to distinguish whether this change is due to a change in resolution or to a change in the actual structure. When nonionic surfactants are studied, it is likely that adsorption also occurs on the oxidized silicon tip, and in general adsorption in the thin film between the tip and sample may be different from adsorption on the isolated surfaces. Thus for nonionic surfactant adsorption, the adsorbed state and the resolution may change together.

Figures 3, 4, and 5 show the force in surfactant solution between a silicon tip and the silica, hydrophobic DEOS-silica, and graphite substrates, respectively. In every case, the force is predominantly repulsive. There are no cases of the strong attractive forces that are characteristic of forces between monolayer surfactant films when the hydrocarbon tails are in contact with water (hydrophobic forces).<sup>14</sup> Thus measurements on all the substrates are consistent with the positioning of

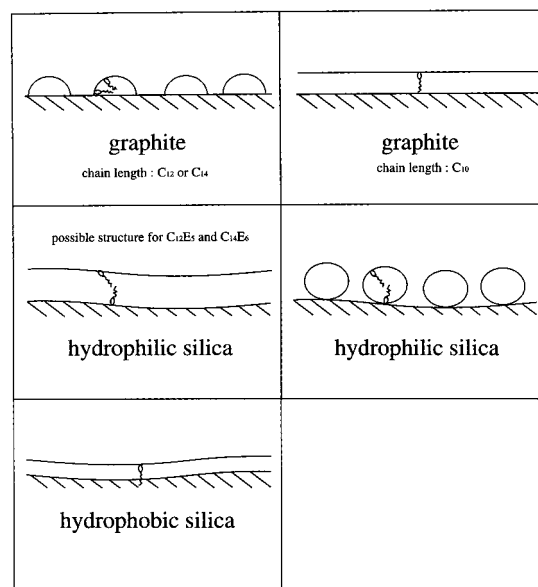


**Figure 6.** Schematic of adsorbed-surfactant structures consistent with AFM images. On graphite, there is a large perturbation from the solution structure caused by high  $\gamma_{\text{graphite-water}}$ , which causes the aggregates to flatten out to cover more of the interface, and a very low  $\gamma_{\text{graphite-hydrocarbon}}$  in a particular orientation, which causes the first layer of surfactant to align with the graphite. The second factor is dominant for longer hydrocarbon chains. On the hydrophilic substrate, there is only a small perturbation of solution structure because water and the micelle have a similar interaction with the solid, whereas on the hydrophobic substrate, the structure is highly perturbed from the solution structure due to the large  $\gamma_{\text{SL}}$ .

hydrophilic ethylene oxide group of the outer surfactant layer in contact with the water as shown in Figure 6.

When imaged at low force on hydrophobic DEOS-silica, all the surfactants produce images that are laterally homogeneous. However, when the force is increased, some amorphous features are imaged, and when the force is increased further, holes appear in the structure (Figure 7). These holes are sometimes correlated with lumps in the underlying substrate. In this case it appears reasonable that the change in structure with force is due to the disruption of the film under the applied load of the tip. The force curves for all the PEO surfactants are quite similar: a repulsive force that begins at about 6 nm and continues to about 2.5 nm (Figure 4). For all cases, the range of repulsive force is greater than the thickness of film measured by ellipsometry<sup>8</sup> and is close to the extended length of the molecule. A fully extended molecule can be discounted because the area per molecule is about 3 times that of a close packed hydrocarbon chain ( $0.59 \text{ nm}^2 \text{ molecule}^{-1}$  vs  $0.20 \text{ nm}^2 \text{ molecule}^{-1}$ ),<sup>8</sup> so full extension would necessitate water mixing with the hydrocarbon chains. It is possible that the extra force-range is due to hydration and protrusion forces, but it is difficult to make an accurate estimate because simultaneous compression and desorption of surfactant may be occurring on the tip. Our work on silica suggests that there is adsorption to the tip, so the force curve represents compliance due to the adsorption on the tip in addition to the substrate.

On hydrophilic silica the situation is more complex because some force curves have two repulsive walls, and the measured adsorbate symmetry is sometimes different at the two positions (Figure 8). Globular micelles were always observed for  $C_{10}E_5$ ,  $C_{10}E_6$ ,  $C_{12}E_8$ , and  $C_{16}E_6$ . Often there were two stable imaging positions, one at a separation of about 3 nm and the other at about 8 nm, but globular features were always observed at both positions. The results for  $C_{12}E_5$  and  $C_{14}E_6$  were unusual. For

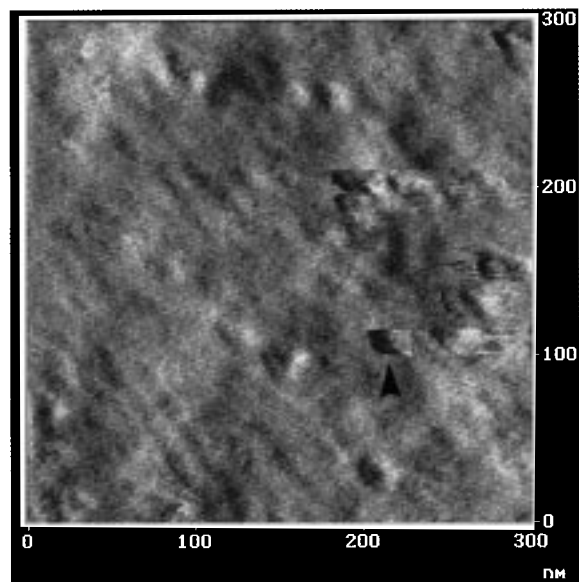


**Figure 7.**  $C_{12}E_5$  on hydrophobic DEOS-silica under a high force. When the force applied to a PEO surfactant on hydrophobic DEOS-silica is increased, the flat layer begins to have a slightly mottled appearance, but on a larger scale (10–20 nm) than the features observed on hydrophilic silica. At a force slightly less than that required for tip instability, the tip occasionally penetrates the film. The arrow indicates an example of this.

$C_{14}E_6$ , a laterally homogeneous structure was observed at large separation (9 nm), and globular aggregates were seen at small separations (3 nm). For  $C_{12}E_5$ , the results were not reproducible, sometimes showing just globular aggregates, sometimes a laterally homogeneous layer, and sometimes a homogeneous layer at large separation and globular aggregates at small separations.

We have also investigated whether the adsorbed structure changes with time since the silica was exposed to surfactant. There was no change in structure in the range 15 min to 3 h after exposure to the surfactant solution. However, the results were somewhat irreproducible if the silica was not exposed to water or water vapor for some time before adsorption of surfactant.

On graphite, the force curves were also complex (Figure 5). Repulsive forces were measured at separations greater than what would be expected from adsorption isotherms,<sup>15</sup> suggesting that the force is influenced by structures on the tip or structures forming in the thin film between the tip and the sample. Previously it has been suggested that graphon (graphitic powdered carbon) can nucleate a phase change in bulk solution.<sup>16</sup> The fact that we measure structure at large tip–sample separations (8–10 nm) provides some evidence that the phase is different in the thin film between the tip and sample than in bulk solution. On graphite, stable imaging positions were often observed at a separation of about 0.3–0.4 nm. This is consistent with a layer of more strongly adsorbed hydrocarbon chains lying in contact with and parallel to the graphite surface. Figure 5 shows that the force required to eject the surfactant from this layer is much greater for  $C_{14}E_6$  than for  $C_{10}E_6$ . This is consistent with a stronger templating effect of the first layer of surfactant for the longer alkyl surfactants.

## Discussion

Our results show that all the surfactants investigated form a laterally homogeneous layer on the hydrophobic DEOS-silica.

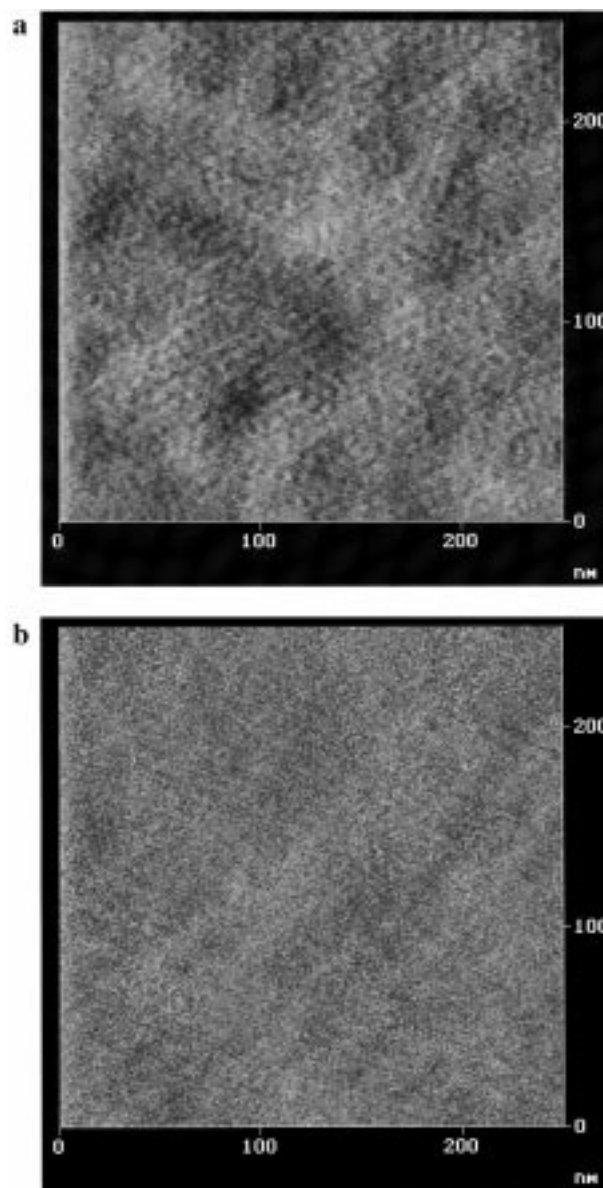


**Figure 8.** Symmetry of the constant-force surface measured by AFM above the  $C_{14}E_6$  layer on hydrophilic silica as a function of the imaging force. (a) At small separations (2–4 nm) and higher forces, the image has features with appropriate dimensions for micelles ( $7.3 \pm 0.5$  nm center-to-center distance and 2–4.5 nm in height.) (b) At larger separations (7.5–9.5 nm), the image is featureless.

This is a major perturbation from the solution-micelle structure. The driving force for this change is probably a reduction in the solid–liquid interfacial energy: a layer that is continuous in two dimensions reduces the free energy by covering the entire high-energy water–solid interface. It is interesting to note that at moderate force, the constant-force surface that we image on top of the surfactant is actually smoother than the chemisorbed diethyloctylchlorosilane layer. The hydrophobic substrate not only causes a lower curvature structure than in solution but also produces an interface that is smoother than itself. To form a flat layer, either it must force the headgroups closer together (by exerting a larger force than the charge–charge and/or hydration forces between the headgroups) or the effective volume occupied by the hydrocarbon must change shape. Tiberg's measurement of the surface excess for  $C_{14}E_6$  shows that the headgroups are not close packed.<sup>8</sup> Together with our results this shows that either the hydrocarbon chains must mix with the diethyloctylchlorosilane layer or the surfactant hydro-

carbon tails adopt a less extended conformation than in micelles. In terms of the packing parameter model,<sup>13</sup> the hydrocarbon tails move from a conical to a cylindrical shape in response to the high solid–water interfacial energy.

In the Results section, we report imaging a flat, continuous layer for C<sub>12</sub>E<sub>5</sub> and C<sub>14</sub>E<sub>6</sub> on hydrophilic silica at 7–9 nm and 8–9 nm tip–sample separations, respectively. This result, together with a repulsive force curve is consistent with the formation of a bilayer-type structure of surfactant at the silica surface (Figure 6). We believe that this structure is most likely to correspond to the structure in the absence of the tip because this is the least intrusive measurement (low force, most distant contact). However, the fact that the structure changes on application of pressure (and thinning of the film) makes it difficult to eliminate the possibility of tip-induced effects when the flat layer is observed.

Tiberg<sup>8</sup> found that C<sub>12</sub>E<sub>5</sub> adsorbed to hydrophilic silica at higher densities than C<sub>12</sub>E<sub>8</sub>. He attributed this behavior to a flat layer caused by the high hydrophobicity of C<sub>12</sub>E<sub>5</sub> compared to C<sub>12</sub>E<sub>8</sub> (high *n:m* ratio). In terms of the packing parameter model, the increased volume of the hydrocarbon chains that must be encapsulated by the headgroups leads to a less curved aggregate. This evolution is also reflected in the bulk-phase behavior of these surfactants: C<sub>12</sub>E<sub>5</sub> has a large lamellar region at 25 °C, but C<sub>12</sub>E<sub>8</sub> has a very small lamellar region, which exists mainly below 25 °C.<sup>17</sup> The surfactant at the interface is much more concentrated than in bulk solution so it is reasonable to expect some correspondence of surface structures to bulk structures at a higher concentration.<sup>3</sup> However, a molecular explanation using the packing parameter model or a correlation with *n:m* ratios does not explain the behavior of C<sub>16</sub>E<sub>6</sub> at the interface. C<sub>16</sub>E<sub>6</sub> has an even higher *n:m* ratio than C<sub>12</sub>E<sub>5</sub> and it has a longer alkyl chain than C<sub>14</sub>E<sub>6</sub> yet it forms globular structures at all forces on the surface. Thus we are not able to provide a broadly applicable molecular explanation of the surface-phase behavior of the C<sub>*n*</sub>E<sub>*m*</sub> surfactants on silica. However, there is no lamellar phase in bulk solution for C<sub>16</sub>E<sub>6</sub> at room temperature, so there is a correlation between the presence of a lamellar phase in bulk solution and a continuous layer at the surface at the same temperature.

On hydrophilic silica, regardless of the structure imaged at large separation (6–10 nm), we usually imaged globular objects at small separations. These globular objects have the same distribution on the silica as the micelles in the thicker films. This suggests that they may be a residue of a thicker structure. For many years it has been proposed that, at concentrations much below the cmc, surfactants aggregate into small clusters held together by the hydrophobic effect.<sup>18</sup> These aggregates are known as hemimicelles. We suggest that the globular structures we observe at small separations are hemimicelles that have adsorbed with the ethylene oxide groups bound to the silica. These hemimicelles could act as nuclei for the adsorption of monomers or are the anchor point for an adsorbed micelle. Because they hydrogen bond to the silica, they remain in the thin film under loads that have displaced surfactant molecules held to the surface via the hydrophobic effect.

The adsorption of an uncharged surfactant to a substrate produces conditions that are good for imaging the substrate. The addition of uncharged, hydrophilic surfactant produces a weak attractive van der Waals force and introduces a short-range repulsive force that is softer than the Pauli exclusion force yet still has a reasonably high gradient. The friction is also very low. The conditions of low friction and a range of stable,

moderate gradient forces near the surface are good for imaging, so it may be useful to image difficult substrates in a surfactant solution above the cmc. The introduced surface features are usually very small, approximately 3 nm, so this preparative technique could be used for lower resolution imaging or with surfactants that naturally form flat layers (double-chained surfactants).

## Conclusions

A wide variety of nonionic surfactants form globular micelles on hydrophilic silica and laterally continuous layers on hydrophobic silica. The structure on hydrophilic silica is similar to that formed in bulk above the cmc, probably because the silica surface contains hydroxyl groups, which can in some ways substitute for the hydrogen bonds of water. The structure on hydrophobic DEOS-silica is a large perturbation of the solution structure, probably because the substrate introduces a new energy term: a minimization of substrate–water area. Mixing of the surfactant and diethyloctylsilane hydrocarbon chains may also contribute to the change in shape from the solution structure. A variety of other surfactants (ionic and zwitterionic) also form lower curvature aggregates on hydrophobic silica.

Most surfactants form hemicylindrical structures on graphite. C<sub>10</sub>E<sub>*m*</sub> surfactants do not. This suggests that there is probably a specific attractive interaction between graphite and alkyl chains that increases in magnitude with the number of methylene units. Thus, longer chain surfactants adsorb epitaxially and template the adsorption of the remainder of the surface aggregate, and shorter chains adsorb so as to cover the maximum area of the hydrophobic graphite interface, producing a flat sheet structure.

**Acknowledgment.** Our thanks go to George Petersen for providing the ultralevers and to Reuben Lamont for preparing the LiFOS.

## References and Notes

- (1) Clint, J. H. *Surfactant Aggregation*; Chapman and Hall: New York, 1992; Chapter 9.
- (2) Grant, L. M.; Ducker, W. A. *J. Phys. Chem.* **1997**, *27*, 5337–5345.
- (3) Ducker, W. A.; Grant, L. M. *J. Phys. Chem.* **1996**, *100*, 11507–11511.
- (4) Manne, S.; Gaub, H. E. *Science* **1995**, *270*, 1480–1482. Manne, S.; Cleveland, J. P.; Gaub, H. E.; Stucky, G. D.; Hansma, P. K. *Langmuir* **1994**, *10*, 4409–4413.
- (5) Patrick, H. N.; Warr, G. G.; Manne, S.; Akasay, I. A. *Langmuir* **1997**, *13*, 4349–4356.
- (6) Cry, D. M.; Venkataraman, B.; Flynn, G. W. *Chem. Mater.* **1996**, *8*, 1600–1615.
- (7) Wanless, E. J.; Ducker, W. A. *J. Phys. Chem.* **1996**, *100*, 3207–3214.
- (8) Tiberg, F. *J. Chem. Soc., Faraday Trans.* **1996**, *92*, 531–538.
- (9) Binnig, G.; Quate, C.; Gerber, G. *Phys. Rev. Lett.* **1986**, *56*, 930–933.
- (10) Cleveland, J. P.; Manne, S.; Bocek, D.; Hansma, P. K. *Rev. Sci. Instrum.* **1993**, *64*, 403–405.
- (11) Ducker, W. A.; Senden, T. J.; Pashley, R. M. *Langmuir* **1992**, *8*, 1831–1836.
- (12) Ducker, W. A.; Wanless, E. J. Submitted to *Langmuir*.
- (13) Israelachvili, J. N. *Intermolecular and Surface Forces*, 2nd ed.; Academic Press: San Diego, 1992; Chapter 17.
- (14) Pashley, R. M.; McGuigan, P. M.; Ninham, B. W.; Evans, D. F. *Science* **1985**, *229*, 1088–1089.
- (15) Corkhill, J. M.; Goodman, J. F.; Tate, J. R. *Trans. Faraday Soc.* **1966**, *62*, 979.
- (16) Clint, J. H. *Surfactant Aggregation*; Chapman and Hall: New York, 1992; p 206.
- (17) Mitchell, D. J.; Tiddy, G. J. T.; Waring, L.; Bostock, T.; McDonald, M. *J. Chem. Soc., Faraday Trans. 1* **1983**, *79*, 975–1000.
- (18) Somasundaran, P.; Fuerstenau, D. W. *J. Phys. Chem.* **1966**, *70*, 90.